

SCIENTIFIC REPORTS

OPEN

MicroRNAs distribution in different phenotypes of Aortic Stenosis

Iacopo Fabiani¹, Nicola Riccardo Pugliese¹, Enrico Calogero¹, Lorenzo Conte¹, Maria Chiara Mazzanti³, Cristian Scatena², Claudia Scopelliti³, Elena Tantillo³, Matteo Passiatore², Marco Angelillis¹, Giuseppe Antonio Naccarato², Rossella Di Stefano¹, Anna Sonia Petronio¹ & Vitantonio Di Bello¹

Received: 5 October 2017

Accepted: 22 May 2018

Published online: 02 July 2018

Aortic valve stenosis (AVS) represents a cluster of different phenotypes, considering gradient and flow pattern. Circulating micro RNAs may reflect specific pathophysiological processes and could be useful biomarkers to identify disease. We assessed 80 patients (81, 76.7–84 years; 46, 57.5% females) with severe AVS. We performed bio-humoral evaluation (including circulating miRNA-1, 21, 29, 133) and 2D-echocardiography. Patients were classified according to ACC/AHA groups (D1-D3) and flow-gradient classification, considering normal/low flow, (NF/LF) and normal/high gradient, (NG/HG). Patients with reduced ejection fraction were characterized by higher levels of miRNA1 ($p = 0.003$) and miRNA 133 ($p = 0.03$). LF condition was associated with higher levels of miRNA1 ($p = 0.02$) and miRNA21 ($p = 0.02$). Levels of miRNA21 were increased in patients with reduced Global longitudinal strain ($p = 0.03$). LF-HG and LF-LG showed higher levels of miRNA1 expression ($p = 0.005$). At one-year follow-up miRNA21 and miRNA29 levels resulted significant independent predictors of reverse remodeling and systolic function increase, respectively. Different phenotypes of AVS may express differential levels and types of miRNAs, which may retain a pathophysiological role in pro-hypertrophic and pro-fibrotic processes.

Aortic valve stenosis (AVS) involves about one-fourth of all patient with chronic valvular heart disease^{1,2}. It is due to a degenerative calcification process of the aortic cusps and, most commonly, it is a slowly progressive active process, associated with significant Left Ventricular (LV) pressure overload, inducing hypertrophy (LVH) and secondary myocardial fibrosis (MF)³. The key findings on transthoracic echocardiogram (TTE) are generally limited to the evaluation of thickening, calcification, reduced systolic opening of the valve leaflets and to flow-dependent parameters assessment (i.e. velocity and gradients), reflecting only the “valvular side” of the pathology⁴. This approach disregards the LV components (function; texture) of the disease, resulting prone to diagnostic discrepancies^{5,6}. Recently in literature, in fact, AVS has been depicted as a complex cluster of different phenotypes. Latest classifications are proposing a central role for indexed stroke volume (SVi) (“flow pattern”) to overcome diagnostic inconsistencies^{7,8}. With respect to this, recent AHA/ACC guidelines for VHD patients management describe 3 distinct phenotypes for symptomatic severe (D) AVS: high gradient (D1); low-flow/low-gradient AVS with reduced Ejection Fraction (EF < 50%), or classical low flow AVS (D2); paradoxical low-flow/low-gradient AVS (D3) (EF > 50%)⁹. Another accredited classification for AVS is based on flow and gradient patterns, identifying 4 groups (group 1: normal flow/low gradient [NF/LG]; group 2: normal flow/high gradient [NF/HG]; group 3: low flow/high gradient [LF/HG]; group 4: low flow/low gradient [LF/LG])^{10,11}. Nowadays, cardiac imaging methods and novel biomarkers could provide an integrated assessment of the functional and structural aspects in AVS. In particular, Speckle Tracking Echocardiography (2D-STE) for the evaluation of myocardial deformation represents a more sensible tool to detect cardiac contractile function abnormalities compared to traditional parameters (i.e. EF)¹². Regarding biomarkers, microRNAs (miRNAs) are small non-coding RNAs of about 21-nucleotides that regulate gene expression at a post-transcriptional level. About 2600 miRNAs have been identified in humans, possibly targeting about 30% of human genes^{13,14}. Specific targets and biological roles have been assigned to only a few miRNAs, although almost every investigated process can be potentially regulated by miRNAs. The expression of many miRNAs shows tissue-specific or stage-specific patterns and their expression is associated with multiple pathological processes (remodeling, hypertrophy, and fibrosis), which have non-negligible effects on the whole

¹Cisanello Hospital AOUP -Department of Surgical, Medical, Molecular Pathology and Critical Area, University of Pisa, Pisa, Italy. ²Department of Translational Research and new technologies in Medicine and Surgery- University of Pisa, 56100, Pisa, Italy. ³Fondazione Pisana per la Scienza, 56100, Pisa, Italy. Iacopo Fabiani and Nicola Riccardo Pugliese contributed equally to this work. Correspondence and requests for materials should be addressed to E.C. (email: enrico.calogero@gmail.com)

cardiovascular system^{13,14}. The presence of circulating non-coding RNAs could be related to specific cardiovascular diseases and may represent a useful biomarker for different cardiovascular diseases identification. Considering the pathophysiological implications of AVS on myocardium (hypertrophy) and interstitium (fibrosis, hypertrophy), we selected from literature a pool of microRNAs with an already proved and extensively demonstrated pro-fibrotic (miRNA21) or pro-hypertrophic (miRNA1, 29, 133) modulatory effect at pre-clinical (*in vitro*/tissue) and clinical level (circulating compartment) on both myocardium and interstitium^{15,16}.

The aim of our study was to evaluate:

- a) the relative expression of miRNA levels in different phenotypes of severe AVS;
- b) the association of miRNA levels with structural and functional echocardiographic variables

in a cohort of patients with severe symptomatic AVS evaluated for aortic valve replacement (AVR).

Materials and Methods

Study population. Eighty patients with severe symptomatic AVS were prospectively enrolled at the AOUP Cardio-Angiology Unit - Pisa and screened between October 2015 and September 2016. For clinical symptoms, a NYHA Class > II was defined as overt heart failure (HF). Patients underwent laboratory analysis (including miRNA assays), and trans-thoracic echocardiography (standard and 2D-STE). The research was carried out according to the code of ethics of the World Medical Association (Declaration of Helsinki), informed consent was obtained, and the author's institutional review board (local ethics committee "Azienda Ospedaliero Universitaria Pisana") approved the study. We excluded patients according to the following criteria: age < 18 years old; presence of major comorbidities (i.e. cancer; dialysis treatment; cachexia); not appropriate acoustic window; coronary/ischemic heart disease (including previous acute coronary syndromes or epicardial coronary artery disease, CAD > 50%); pregnancy; moderate or severe valvular disease; inability to sign consent; non-degenerative AVS; diskynetic septum (i.e. pacemaker induced rhythm patients; intraventricular conduction disorders). Follow-up data were collected at 12 months from AVR, using cardiologic visit (outpatient) and echocardiographic exam.

Conventional Echocardiography. We performed complete transthoracic exams using a heart-dedicated machine (Vivid-E80, General Electric Milwaukee, WI-USA). Lateral decubitus position was the selected position while data acquisition was performed with a matrix (M5S) probe at a depth of 16 cm in apical views (two-chamber, four-chamber and apical views) and the parasternal view (short- and long-axis views). All parameters were collected according to current recommendations^{4,17}. Using standard M-mode/2D images at the parasternal long-axis views we calculated LV dimensions, including end-diastolic/end-systolic LV diameters, end-diastolic thickness of the interventricular septum and posterior wall. Body surface area (BSA) was utilized to correct left ventricular mass calculation to derive mass index (LVMI). Both the apical 2- and 4-chamber views were considered to evaluate the LV end-diastolic and end-systolic volumes, and standard Simpson's rule was utilized to calculate EF. A spectral pulsed-wave Doppler analysis was performed to assess LV diastolic function, measuring early (E wave) and late (A wave) trans-mitral velocities, E/A ratio, and E wave deceleration time (DT). TDI was performed, adjusting gain and frame rate to optimize tissue characterization. The continuity equation was used to calculate the aortic valve area indexed (AVAi), and the modified Bernoulli equation allowed the estimation of the maximum pressure gradient across the restrictive orifice. Mean trans-aortic pressure gradient (MG) derived from averaging the instantaneous gradients over the ejection period measured by continuous-wave Doppler recordings. We calculated also the valvulo-arterial impedance (Z_{VA}) as a measurement of global LV afterload¹⁸. We used the color Doppler mode optimizing gain and Nyquist limit to evaluate the presence of regurgitant valve disease. The severity of valvular regurgitation was evaluated using a qualitative scale (mild, moderate, and severe), according to the current guidelines^{4,17}.

In our study population, we adopted the following classification criteria:

- Reduced EF was defined according to guidelines as $EF < 50\%$ ¹⁷;
- Reduced global longitudinal strain (GLS), in accordance with prognostic studies, was defined as a value $> -15.9\%$ ¹⁹;
- Concentric Physiology was defined in presence of a Relative Wall Thickness (RWT) > 0.42 , while relevant hypertrophy in presence of $LVMI > 95 \text{ g/m}^2$ for women and 115 g/m^2 for men²⁰;
- Low transvalvular gradient was defined in presence of a $MG < 40 \text{ mmHg}$ ¹¹;
- Low flow condition was defined in presence of $SVi < 35 \text{ ml/m}^2$ ⁷;
- Abnormal Z_{VA} was considered for values $> 4.5 \text{ mmHg/ml/m}^2$ ¹⁸;
- AHA/ACC classification: D1 (Classical Phenotype: $V_{max} > 4 \text{ m/sec}$; $MG > 40 \text{ mmHg}$; $AVAi < 0.6 \text{ cm}^2/\text{m}^2$), D2 (Classical Low Flow Low Gradient: $V_{max} < 4 \text{ m/sec}$; $MG < 40 \text{ mmHg}$; $AVAi < 0.6 \text{ cm}^2/\text{m}^2$) and D3 (Paradoxical Low Flow Low Gradient: $V_{max} < 4 \text{ m/sec}$; $MG < 40 \text{ mmHg}$; $AVAi < 0.6 \text{ cm}^2/\text{m}^2$, with an $SVi < 35 \text{ ml/m}^2$)⁹;
- Flow-Gradient classification: 1) NF/LG; 2) NF/HG; 3) LF/HG; 4) LF/LG¹¹.

Speckle Tracking Echocardiography. We used 2D-STE (frame rate 45–90 frame/sec, fps) to assess LV GLS, according to current standards²¹. Only the global longitudinal component of strain (peak value-mid myocardium) was considered, using a dedicated software (EchoPAC 12, General Electric). To achieve this aim, we acquired standard 2D grey-scale images of the LV at conventional apical 2-, 4-chamber and apical long-axis views. By

tracking frame-to-frame natural acoustic markers, or speckles, equally distributed within the myocardial wall, 2D-STE represents an angle-independent technology, allowing myocardial deformation analysis. The percentage change in myocardial length relative to the initial length, according to the strain Lagrangian formula, expresses myocardial strain in percentage. Analysing temporal variation of myocardial strain, we are able to calculate the strain rate that represents a measure of deformation rate. The longitudinal deformation consists in motion from mitral annulus to the apex in the apical views and may be negative (shortening) or positive (lengthening). We traced manually the endocardial contour at the end-systolic frame. Then the software, automatically, traced a concentric region of interest (ROI), including the entire myocardial wall. We verified the myocardial tracking, and we adjusted the ROI to optimize the tracking, where needed. Dividing each LV image into 6 segments, we performed a global and segmental strain analysis. A random sample of 10 patients was re-analysed by 2 independent observers. The intraclass correlation coefficient (ICC) and its 95% confidence intervals (CIs) were calculated to evaluate inter- and intra-observer reproducibility of 2D-STE. We obtained a good intra-observer and inter-observer repeatability (ICCs > 0.80).

Invasive Measurements. Standard left heart catheterization was performed before AVR in 60 patients, in addition to coronary angiography. Invasive end-diastolic pressure (EDPi; fluid-filled catheter), peak-to-peak gradient, and semi-quantitative aortic regurgitation were evaluated.

Circulating miRNAs Study. We collected peripheral blood samples in specific tubes (PAXgene Blood RNA Tube), designed for immediate stabilization of peripheral blood RNA (PreAnalytiX). Blood samples were collected and frozen at -80°C within 2 hours after blood test. Frozen samples were equilibrated at room temperature for 2 hours before processing. RNA was isolated using the PreAnalytiX PAXgene miRNA isolation kit according to the manufacturer's protocol. We estimated the quantity of RNA using $2\ \mu\text{l}$ of undiluted RNA solution and a Qubit 2.0 Fluorometer (Life Technologies). The results ranged from 50 to 500 ng/ μl of RNA. miRNAs were reverse transcribed from 500 ng of total extracted RNA sample using the miScript II RT Kit (QIAGEN). miRNA expression analysis was performed three times using $1\ \mu\text{l}$ of cDNA as a template for real-time PCR with the miScript SYBR Green PCR Kit (QIAGEN) and the miScript Primer Assays (SNORD96 - assay code MS00033733, miRNA21 - assay code MS00009079, miRNA1 - MS00008358, miRNA133 - MS00031423, miRNA29 - MS00003269 assay code (QIAGEN)) according to manufacturer's instructions on the CFX96 Real Time system c1000 thermal cycler (BIORAD). Data analysis was performed using the Bio-Rad CFX Manager Software v3.1. miRNA21, miRNA1, miRNA133 and miRNA29 expression was calculated using SNORD96 expression level as reference and the relative normalized expression $\Delta\Delta\text{Cq}$ formula. The number of technical replicates used for miRNA21, miRNA1, miRNA133 and miRNA29 was 3. We reported normalized expression levels respective to a housekeeping gene.

All miRNA expression analyses were adjusted for estimated glomerular filtration rate (eGFR) values.

In 38 subjects (47.5%) (see *Supplementary Material and Table* for details), in order to avoid the potential confounder effect, among others, of circulating blood cells, limiting cardiac specificity of miRNAs here tested, we validated circulating whole blood vs plasmatic compartment by mean of linear regression analysis, also calculating inter-rater correlation coefficients (ICC). In the present paper we did not report a correlation between miRNAs expression levels and circulating blood cells.

Statistical Analysis. The Kolmogorov-Smirnov test for normality was used to assess the data. Continuous variables are presented as mean and 95% confidence intervals if normally distributed or median and range inter-quartile if not normally distributed. Percentage was used for categorical data. We treated the circulating miRNA levels as continuous variables, or we normalized them with Log transformation. Continuous variables were compared using Student's t-test or Mann-Whitney U test when non-Gaussian. Correlation r coefficient (or Spearman's rho) were assessed as appropriate. ANOVA or Kruskal-Wallis test were used to evaluate distribution of miRNA levels in different classification categories, with appropriate post-hoc corrections for interactions. For discrimination of patients with reduced SVi we used a c-statistic approach to derive the miRNA value with the best combination of sensitivity and specificity. Multivariate, stepwise regression analysis was used to identify predictors of reverse remodeling (Model 1) and systolic function recovery (Model 2). In the text we considered GLS in absolute value in order to preserve the statistical meaning of regression analysis (direct/inverse correlation/association). The threshold for statistical significance was $p < 0.05$. The following statistic package was used: Medcalc 12.7 (Medcalc Software 2013, Belgium).

Results

Table 1 summarizes clinical characteristics of our patient population (80 subjects with a confirmed diagnosis of severe AVS), and in Table 2 all the common echocardiographic variables describing AVS are indicated.

In Table 3, normalized expression levels of circulating miRNAs (miRNA1-21-29-133) are specified. Principal characteristics of population are reported in Table 4 according to the ACC/AHA and Flow/Gradient classification (preserved EF).

We observed 14% of patients ($n = 11$) with reduced EF. Circulating miRNA21 showed inverse correlation with GLS in absolute value ($r = -0.3$, $p = 0.009$) and a direct correlation with E/e' ($r = 0.33$, $p = 0.058$; Fig. 1A); miRNA29 had inverse correlation with age ($r = -0.34$, $p = 0.004$), eGFR ($r = -0.37$, $p = 0.02$) and GLS ($r = -0.38$, $p = 0.001$; Fig. 1B); miRNA1 demonstrated inverse correlation with SVi ($r = -0.32$, $p = 0.03$; Fig. 1C) while miRNA133 inverse correlation with DT ($r = -0.39$, $p = 0.001$), EF ($r = -0.45$, $p = 0.002$; Fig. 1D), eGFR ($r = -0.3$, $p = 0.01$), age ($r = -0.3$, $p = 0.01$), and direct correlation with E/A ratio ($r = 0.36$, $p = 0.03$), ESV ($r = 0.44$, $p = 0.002$), sPAP ($r = 0.37$, $p = 0.002$), EDPi ($r = 0.37$, $p = 0.05$). Using a c-Statistic approach, miRNA1 had a Sensitivity of 77% and a Specificity of 68% (AUC 0.7; $p = 0.01$) for discriminating reduced SVi subjects. Levels of miRNA21 were increased in patients with a diagnosis of overt HF (6.68, 2.83–9.81 vs 1.85, 1.01–2.59; $p = 0.01$)

Gender (Male)	34	42%
Age (years)	81	76.7–84.0
Weight (Kg)	73	69.8–75.3
Height (cm)	164	164.2–167.9
BMI (kg/m ²)	26	25.5–27.1
BSA (m ²)	1.8	1.78–1.86
SAP (mmHg)	137.6	133–141
DAP (mmHg)	71.5	68–74
Smokers	11	13.6%
Family history of cerebro-vascular disease	18	22.2%
Diabetes Mellitus	21	25.9%
Hypertension	70	86.4%
Dyslipidaemia	11	13.6%
Obesity	16	19.7%
History of Angina	24	29.6%
CAD (<50% Epicardial Vessels)	35	43.2%
COPD	18	22.2%
NYHA class I/II	48	59.3%
NYHA class >II	33	40.7%
Syncope	9	11.1%
Atrial Fibrillation	9	11.1%
eGFR (mL/min/1.73 m ²)	58.667	46.4–76.1
CKD	46	56.8%
Anaemia	18	22.2%
White Blood Cells (103/μL)	8	5–10.5
Erythrocytes (106/μL)	4	3.5–6
Platelets (103/μL)	180	140–230
EuroSCORE II (%)	2.6	1.7–4.0
Logistic EuroSCORE (%)	8.38	4.7–15.1

Table 1. Clinical characteristics of study population (n = 80), risk factors and comorbidities. Note: the data are presented as number and %, mean and 95% confidence intervals if normally distributed or median and range interquartile if not normally distributed. BMI: body mass index; BSA: body surface area; CAD: coronary artery disease; CKD: chronic kidney disease; COPD: chronic obstructive pulmonary disease; DAP: diastolic arterial pressure; eGFR: estimated glomerular filtration rate; NYHA: New York Heart Association; SAP: systolic arterial pressure.

and reduced GLS (3.45, 1.94–6.6 vs 1.5, 0.71–3.08; $p = 0.03$; Fig. 2A). A reduced SVi was characterized by higher levels of miRNA1 (0.67, 0.12–2.48 vs 0.14, 0.06–0.37; $p = 0.02$; Fig. 2B) and miRNA21 (4.16, 1.98–7.99 vs 1.72, 0.7–2.85; $p = 0.02$). Patients with reduced EF were characterized by significantly higher levels of miRNA1 (0.16, 0.08–0.41 vs 3.3, 0.5–18.02; $p = 0.003$; Fig. 2C) and miRNA133 (7.9, 1.01–16.29 vs 1.03, 0.76–1.68; $p = 0.03$). The presence of significant LVH was associated to higher levels of miRNA133 (1.51, 1.01–4.86, versus 0.64, 0.31–1.33; $p = 0.02$). Distribution of levels of miRNA29 was significantly different when we considered the 3 sub-classes of symptomatic severe AVS (D stage: D1, classical phenotype, 77%, D2, low/flow low gradient with reduced EF, 17%; D3, paradoxical low flow/low gradient 4%; $p = 0.03$, with higher levels for D2). Considering the flow/gradient classification of AS, we observed 14 patients (21.2%) with normal SVi/low MG; 32 (37.5%) with normal SVi/high MG; 13 (16.2%) with low SVi/high MG; 4 (3.8%) with low SVi/low MG. Only miRNA1 showed a significant different distribution in the groups, with higher values for group 3 and 4 (Overall p for ANOVA = 0.005; 1 vs 2 $p = ns$; 3 vs 2 $p = 0.05$; 3 vs 1 $p = 0.001$; 3 vs 4 $p = ns$; 4 vs 1 $p < 0.0001$; 4 vs 2 $p = 0.005$ Fig. 2D). There were no age-related, gender, or ethnic differences in study population.

Follow-up. Follow-up data were available in 75 subjects (94% of cases). Thirty patients underwent surgical valve replacement (37.5%, of which 25 [83%] with a biologic prosthesis), while 50 (62.5%) underwent percutaneous procedure. After an average follow-up of 15 ± 3 months, no major procedural complications nor long-term cardio-vascular events were noted. An increase in AVAi was observed (baseline AVAi 0.36 cm², 95% CI 0.33–0.38 vs follow-up 1.5 cm², 95% CI 1.36–1.6; $p < 0.0001$; Delta AVAi 1.02, 95% CI 0.93–1.11 cm²), as well as a reduction in peak trans-valvular velocity (baseline Vmax 4 m/sec, 95% CI 4.3–4.5 vs follow-up 2.1 m/sec, 95% CI 2–2.28; $p < 0.0001$; Delta V max 2.12, 95% CI 2.01–2.35 m/sec). A significant reverse remodeling was also observed (baseline LVMi 134 g/m², 95% CI 127.3–140 vs follow-up 119.6, 95% CI 114.6–124.5; $p < 0.0001$; Delta LV mass indexed 16.07, 95% CI 6.77–25.38 g/m²). No significant increase in EF was reported (baseline EF% 61, 95% CI 54.7–68.1 vs follow-up 62, 95% CI 55.5–69; $p = ns$; Delta EF 2.34, 95% CI –1.45–6.17%), while GLS significantly improved from baseline (baseline GLS% –14, 95% CI 13.2–14.7 vs Follow-up –15.6, 95% CI 14.7–16.4; $p = 0.01$;

LV EDVi (ml/m ²)	48	40.6–58.6
LV ESVi (ml/m ²)	24	16.9–33.0
IVS (mm)	13	12–14
RWT	0.508	0.488–0.527
LAVi (cm ² /m ²)	44	40.6–47.3
E/A	0.729	0.55–1.05
DT (ms)	232	215.2–248.4
E/e' (average sept + lat/2)	17	15.1–18.3
s' septal (cm/s)	6	5.3–6.0
s' lateral (cm/s)	6	5.0–7.4
EF (%)	61	54.7–68.1
GLS (%)	–14	13.2–14.7
LVMi (g/m ²)	134	127.3–139.9
LVH	73	91.2%
Estimated sPAP	30	25–35
Systolic dysfunction (EF < 50%)	14	17%
Diastolic dysfunction (grade I/II/III)	13/47/20	16.3/58.7/25%
Stroke Volume index (ml/m ²)	35	33.1–37.7
AVAi (ml/mq)	0.359	0.33–0.38
AS jet velocity (m/s)	4	4.29–4.50
Maximum pressure gradient (mmHg)	77	69.0–87.8
Mean pressure gradient (mmHg)	47	41.0–53.8
Velocity Ratio	0.202	0.19–0.21
ZVA (mmHg/mL/m ²)	5	4.280–6.06
TAPSE (mm)	20	17.75–24
ACC/AHA GROUP: D1/D2/D3	62/14/4	77.5%/17.5%/5%
FLOW/GRADIENT GROUP: NF-LG/ NF-HG/LF-HG/LF-LG	17/32/13/4	21%/40%/16%/4%

Table 2. Echocardiographic parameters. Note: the data are presented as number and %, mean and 95% confidence intervals if normally distributed or median and range interquartile if not normally distributed. ACC/AHA: American College of Cardiology/American Heart Association group: D1) Classical Phenotype ($V_{max} > 4$ m/sec; $MG > 40$ mmHg; $AVA_i < 0.6$ cm²/m²); D2) Classical Low Flow Low Gradient ($V_{max} < 4$ m/sec; $MG < 40$ mmHg; $AVA_i < 0.6$ cm²/m²); D3) Paradoxical Low Flow Low Gradient ($V_{max} < 4$ m/sec; $MG < 40$ mmHg; $AVA_i < 0.6$ cm²/m², with an $SV_i < 35$ ml/m²). FLOW/GRADIENT GROUP: NF normal flow ($SV_i > 35$ ml/m²); LF low flow ($SV_i < 35$ ml/m²); LG low gradient (mean pressure gradient < 40 mmHg); HG high gradient (mean pressure gradient > 40 mmHg). AS: aortic stenosis; AVA_i : aortic valve area index; DT: deceleration time; E/A: ratio of early to late diastolic mitral filling velocity (PW); EDVi: indexed end-diastolic volume; E/e': ratio of trans-mitral early diastolic velocity (PW) to tissue early diastolic mitral annular velocity (TDI); EF: ejection fraction; ESVi: end-systolic volume indexed; GLS: global longitudinal strain; IVS: inter-ventricular septum; LAVi: indexed left atrium volume; LVMi: indexed left ventricular mass; LV: left ventricle; LVH: left ventricular hypertrophy (defined as $LVM_i > 115$ g/m² in males or > 95 g/m² in females); sPAP systolic pulmonary artery pressure; RWT: relative wall thickness; TAPSE: tricuspid annular plane systolic excursion; ZVA: valvulo-arterial impedance.

microRNA	Normalized Expression Levels	95%CI	Number of Experimental Replicates
miRNA1	0.262	0.0733–1.399	3
miRNA133	1.324	0.637–10.236	3
miRNA29	1.256	0.535–8.042	3
miRNA21	2.471	0.867–8.012	3

Table 3. Relative expression levels of circulating miRNAs. Note: the data are presented as number, mean and 95% confidence intervals if normally distributed or median and range interquartile if not normally distributed.

Delta GLS in absolute value 0.52, 95% CI 0.21–0.72%). A significant correlation between Delta AVA_i and Delta GLS was found ($r = 0.33$; $p = 0.01$). In a multivariate stepwise regression model (Table 5a), using reverse remodeling (LV Mass Reduction) as a dependent variable, miRNA21 levels resulted significant independent predictors with baseline eGFR and Delta V_{max} ($R^2 = 0.89$), while, in another model (Table 5b), miRNA29 baseline levels and Delta AVA_i emerged as independent predictors of Delta GLS ($R^2 = 0.58$). No significant gender differences were monitored during follow-up data.

Variable	Flow/Gradient Groups				p	Acc/Aha Groups			
	NF/LG (17)	NF/HG (32)	LF/HG (13)	LF/LG (4)		D1 (62)	D2 (14)	D3 (4)	p
Gender (% of female)	43%	50%	87%	33%	0.01	63%	29%	67%	0.05
E/e' average	15.6 (9.2–22)	15.7 (14–18)	18.2 (14.5–22)	19.3 (16.5–22)	ns	15.3 (15.6–19)	15.6 (12.3–18.4)	17 (15.2–18)	ns
AGE, years	78 (67–88)	78 (74–81)	80 (78–82)	81 (79–84)	ns	79.4 (77.5–81)	78.1 (72.3–84)	79.3 (73–87)	ns
EDVi, ml/m ²	52 (44.5–59)	52 (48–56)	46 (43–48.7)	45 (41–48)	0.01	49.2 (46–52.3)	70 (53–84)	48.2 (41–64)	<0.0001
EF%	62 (54–71)	68 (65–70)	63 (61–66)	60 (55–66)	ns	63 (59.5–65.2)	49 (40.7–53.1)	60 (57.5–61.3)	0.01
GLS%	−16.3 (13.8–17)	−15.3 (14–16.4)	−14.4 (12.9–15.9)	−11.5 (10–15.5)	ns	−14.5 (13.6–15)	−10 (9.5–12.3)	−13 (10.7–14.7)	0.05
LAVi, ml/m ²	41.4 (31.8–55)	43.7 (38.1–49)	46 (38.2–52)	47 (41–55)	ns	45 (41–48.7)	43 (36–49)	35 (28.2–38)	ns
LVMi, g/m ²	131 (94–160)	127 (116–137)	127 (118–135)	133 (114–143)	ns	132 (125–138)	145 (127–155)	136 (89–155)	ns
RWT	0.5 (0.44–0.57)	0.5 (0.45–0.55)	0.54 (0.50–0.57)	0.55 (0.51–0.57)	ns	0.51 (0.5–0.54)	0.44 (0.4–0.5)	0.54 (0.46–0.58)	0.005
ZVA, mmHg/ml/m ²	4.4 (3.4–5.3)	4.6 (4–5.2)	5.5 (5.1–5.8)	6.1 (5.5–6.3)	0.01	5.2 (4.8–5.5)	4.8 (4.2–5.5)	5.5 (4.6–6)	ns

Table 4. Distribution of the principal variables according to ACC/AHA and Flow/Gradient classification. Note: the data are presented as number and %, mean and 95% confidence intervals if normally distributed or median and range interquartile if not normally distributed. ACC/AHA: American College of Cardiology/American Heart Association group; D1) Classical Phenotype ($V_{max} > 4$ m/sec; $MG > 40$ mmHg; $AVA_i < 0.6$ cm²/m²); D2) Classical Low Flow Low Gradient ($V_{max} < 4$ m/sec; $MG < 40$ mmHg; $AVA_i < 0.6$ cm²/m²); D3) Paradoxical Low Flow Low Gradient ($V_{max} < 4$ m/sec; $MG < 40$ mmHg; $AVA_i < 0.6$ cm²/m², with an $SV_i < 35$ ml/m²). FLOW/GRADIENT GROUP: NF normal flow ($SV_i > 35$ ml/m²); LF low flow ($SV_i < 35$ ml/m²); LG low gradient (mean pressure gradient < 40 mmHg); HG high gradient (mean pressure gradient > 40 mmHg). EDVi: indexed end-diastolic volume; E/e': ratio of trans-mitral early diastolic velocity (PW) to tissue early diastolic mitral annular velocity (TDI); EF: ejection fraction; GLS: global longitudinal strain; LAVi: indexed left atrium volume; LVMi: indexed left ventricular mass; RWT: relative wall thickness; ZVA: valvulo-arterial impedance.

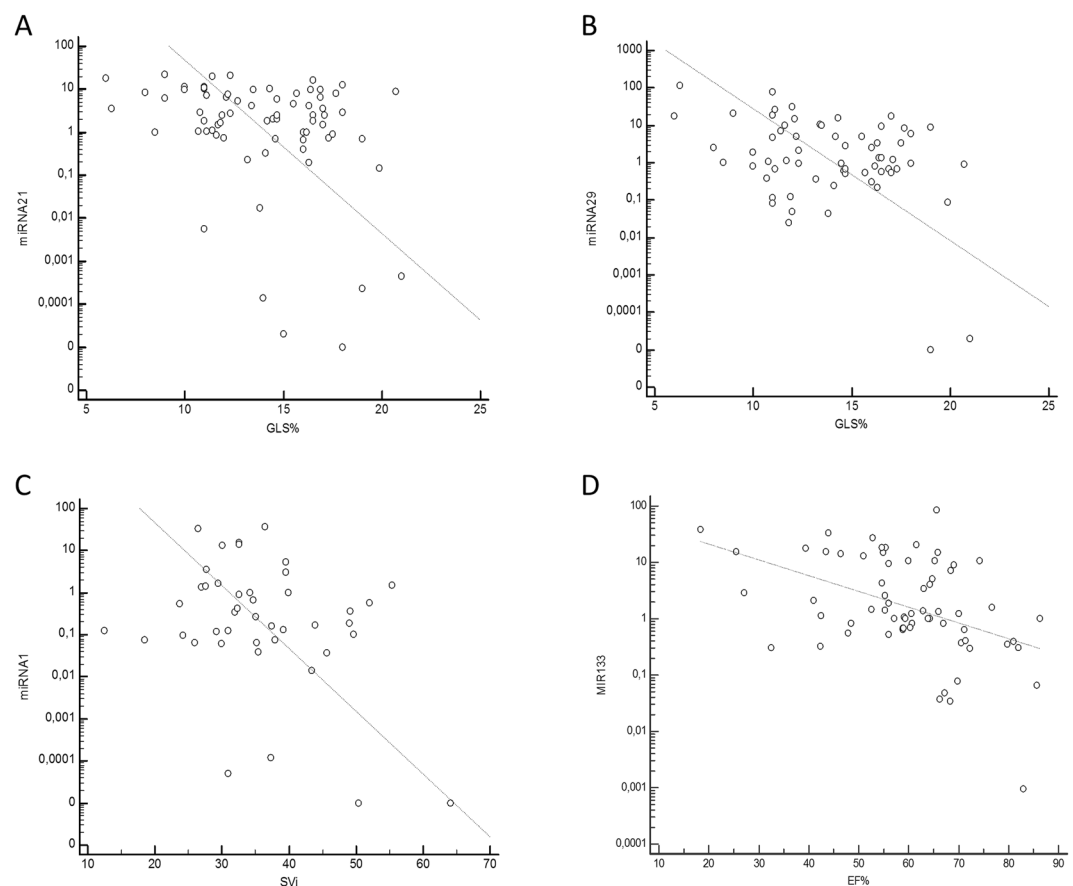


Figure 1. Correlation analysis. (A) Correlation between global longitudinal strain (GLS, % in absolute value) and microRNA21 (miRNA21, Log Scale): $r = -0.3$, $p = 0.0009$. (B) Correlation between GLS and microRNA29 (miRNA29, Log Scale): $r = -0.38$; $p = 0.001$. (C) Correlation between indexed stroke volume (SV_i , ml/m²) and micro RNA1 (miRNA1, Log Scale): $r = -0.32$; $p = 0.003$. (D) Correlation between ejection fraction (EF%) and micro RNA133 (miRNA133, Log Scale): $r = -0.45$; $p = 0.002$.

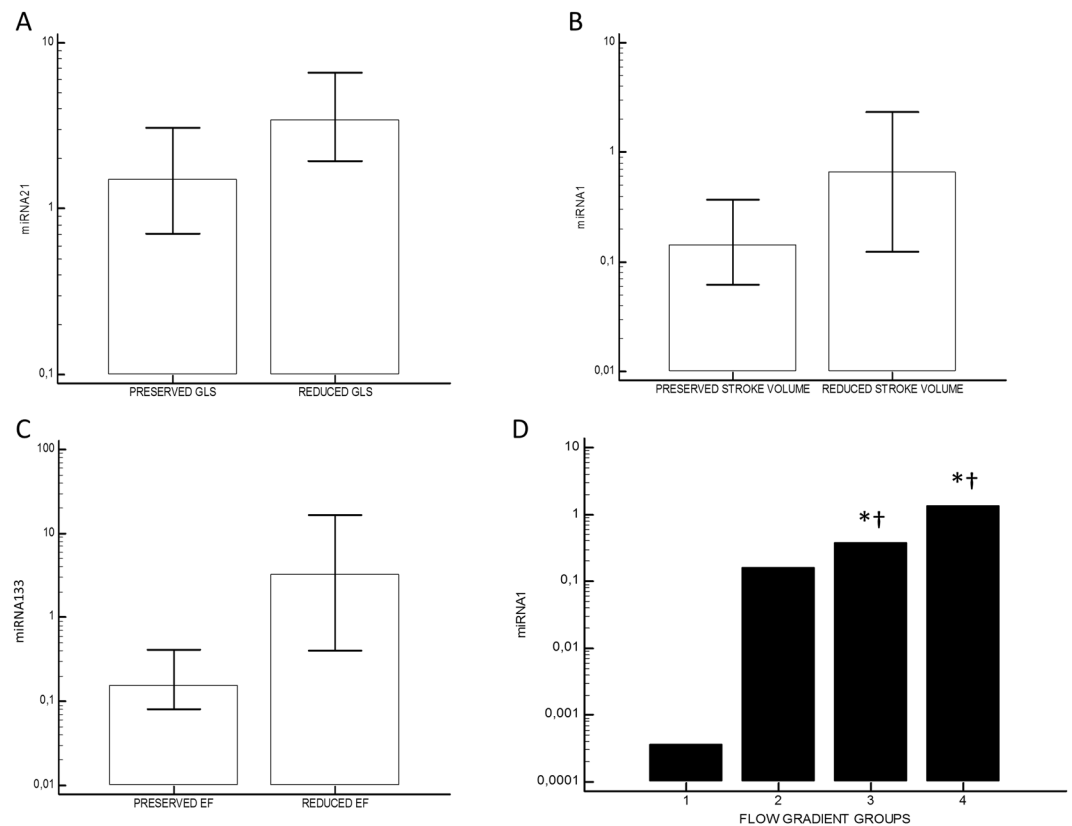


Figure 2. Differential distribution of miRNA expression levels. (A) miRNA21 in patients with reduced vs preserved global longitudinal strain (GLS, cut-off: -15.9%): 3.45, 1.94–6.6 vs 1.5, 0.71–3.08; $p = 0.031$. (B) miRNA1 in patients with reduced vs preserved stroke volume indexed (cut-off: 35 ml/min): 0.67, 0.12–2.48 vs 0.14, 0.06–0.37; $p = 0.02$. (C) miRNA133 in patients with reduced vs preserved ejection fraction (EF, cut-off: 50%): 7.9, 1.01–16.29 vs 1.03, 0.76–1.68; $p = 0.03$. (D) miRNA1 distribution according to flow-gradient classification (Group 1: Normal Flow/Low Gradient; Group 2: Normal Flow/High Gradient; Group 3: Low Flow/High Gradient; Group 4: Low Flow/Low Gradient). * $p < 0.05$ in comparison with group 1; † $p < 0.05$ in comparison with group 2.

Independent variables	Coefficient	Std. Error	r_{partial}	t	p
a. Regression model: Delta LV Mass					
(Constant)	376.6904				
eGFR (mL/min/1.73 m ²)	0.3180	0.1435	-0.5095	-2.216	0.0438
miRNA21	-4.6870	0.9933	-0.7835	-4.718	0.0003
Delta V max (m/sec)	75.3057	6.9720	-0.9449	-10.801	< 0.0001
b. Regression model: Delta GLS					
(Constant)	-0.002970				
miRNA29	-0.07732	0.01347	0.7606	5.739	< 0.0001
Delta AVAi (cm ² /m ²)	0.082	0.01647	0.6606	5.49	< 0.0001

Table 5. Delta LV mass and Delta GLS Multivariate regression model. Note: Delta GLS was considered in absolute value. AVAi: aortic valve area indexed; eGFR: estimated glomerular filtration rate; GLS: global longitudinal strain; LV: left ventricle.

Discussion

Principal findings of our study are

- miRNAs have a differential distribution considering different phenotypes of severe AVS: a low flow condition is associated with increased levels of miRNA21, miRNA1 and miRNA133, while LVH is reflected by higher levels of miRNA133;
- miRNA21 levels reflect both functional and hemodynamic impairment;

- a more advanced stage of AVS, typically characterized by a reduced EF, is associated with higher levels of miRNA29, miRNA133 and miRNA1;
- miRNA21 and miRNA29 result independent predictors of reverse remodelling and systolic function recovery after aortic valve replacement.

Severe AVS is associated with increased hemodynamic load and significant LV remodeling (encompassing hypertrophy and fibrosis), finally leading to impaired myocardial function and poor outcome in the absence of appropriate treatment^{1,3}. However, as previously stated, the main focus of routine evaluation of AVS is the assessment of valvular parameters, with a limited role attributed to LV compartment^{2,4}. Moreover, discrepancies are frequently observed between the parameters, especially when a low-flow state exists as a result of reduced EF or in case of severe LV remodeling despite preserved EF (>50%)^{5,10}. Several papers recently reported the determinant prognostic role of SVi, as a strong indicator of functional and flow conditions: reduced SVi is associated with advanced ventricular remodeling condition and a poor outcome^{6,10,22,23}. Furthermore, LV response in terms of hypertrophy and fibrosis is peculiar in patients with AVS, because several factors (including age, sex, Z_{VA} , bio-modulators) play different roles at different levels and in different stages of the disease^{18,24}. Current knowledge allows us to assert that miRNAs might represent important regulators of valvular disease development. Available data suggest that distinct miRNAs are dysregulated in AVS, supporting different underlying pathophysiological mechanisms. miRNA21 is up-regulated in cardiomyocytes during the fibrotic process; indeed, both myocardial and circulating levels of miRNA21 are significantly higher in patients with AVS compared to controls, correlating with MG and fibrosis. Previous data from our group also showed how miRNA21 manifested both in interstitial tissue and myocytes, with the fibrous tissue representing the site of major expression^{25–27}. In this study, miRNA21 levels are associated with an impaired myocardial deformation, evaluated by GLS, and a reduced SVi, together with altered diastolic function and increased non-invasively-estimated filling pressure. Both miRNA29 and miRNA133 are modulators of fibrotic and hypertrophic processes and may reflect these 2 coexisting conditions also in AVS, potentially identifying an advanced or rapidly progressing valvular disease. In details, miRNA29 family is down-regulated in fibroblasts during myocardial fibrosis while it is up-regulated in myocardial hypertrophy; miRNA133 is down-regulated in cardiomyocytes during myocardial fibrosis and hypertrophy development. Combining the analysis of these modulators together with clinical parameters, it has been possible to predict LV mass normalization at one year after AVR^{28–30}. Indeed, in our study miRNA29 and miRNA133 levels were significantly associated with some of the principal pro-fibrotic conditions (e.g. inverse correlation with eGFR and age), leading to impaired myocardial deformation and increased filling pressures. Interestingly, miRNA29 showed a differential distribution according to ACC/AHA stages of Valvular AS, with significantly higher levels in D2 patients (i.e. low-flow/low-gradient). Previous findings demonstrated both LVH and advanced systolic compromise (namely EF reduction) represent relevant triggers for miRNA133 release³¹. We confirmed these data in our study, showing miRNA133 levels significantly increased in patients with reduced EF and advanced LVH. We focused also on miRNA1, described as down-regulated in cardiomyocytes during myocardial hypertrophic process^{32,33}. In our population, miRNA1 levels increased in presence of reduced SVi and EF, with a significant differential distribution in 4-group flow-gradient classification (with higher levels in LF/HG and LF/LG groups). These findings further emphasize the link between the hypertrophic response and the impaired LV flow and function, proposing miRNA1 as a reliable index of flow condition and ventricular function, especially in AVS. Finally, according to literature, we reported a reduction of LV mass during follow-up (reverse remodeling) and an increase in longitudinal systolic function (GLS)^{12,34}. Interestingly, in our regression models, baseline miRNA 21 and 29 levels resulted predictors of mass reduction, as previously shown³⁰, and systolic function increase, assessed in terms of GLS, respectively. Then, we can speculate that the available evidence baseline miRNA levels may be helpful diagnostic tools in terms of prediction of post-operative LV remodeling.

Limitations

Our population, although significant, could result too limited in number since the multiple phenotypes of AS patients described. Furthermore, a control population for miRNAs was not included. However, previous papers had already shown data on AVS patients vs a normal population, so we mainly aimed at examining a differential miRNA-level distribution in anhomogeneous population (severe symptomatic AVS).

Conclusions

AVS Common characterization cannot fully elucidate the complex pathophysiology of the cardiac remodeling process. Myocardial hypertrophy, fibrosis and apoptosis represent the main actors of cardiac remodeling in AVS: these patterns are regulated not only by pressure overload, but also by a complex network of humoral modulators. Our study aims at proposing a model of translational research in AVS for a better diagnostic and prognostic patient stratification. Different phenotypes of AVS, with variable degrees of functional and hemodynamic impairment, express differential levels and types of circulating miRNAs. In this scenario, miRNAs could supply a more integrated knowledge of the disease and become a marker of fibrosis/adverse hypertrophic stimulus³⁴, even predicting the development of systo-diastolic dysfunction.

References

1. Carabello, B. A. & Paulus, W. J. Aortic stenosis. *Lancet*. **373**, 956–966 (2009).
2. Vahanian, A. *et al.* Guidelines on the management of valvular heart disease (version 2012). *Eur Heart J*. **33**, 2451–2496 (2012).
3. Hein, S. *et al.* Progression from compensated hypertrophy to failure in the pressure-overloaded human: heart structural deterioration and compensatory mechanisms. *Circulation*. **107**, 984–991 (2003).
4. Baumgartner, H. *et al.* Echocardiographic assessment of valve stenosis: EAE/ASE recommendations for clinical practice. *Eur J Echocardiogr*. **10**, 1–25 (2009).

5. Minners, J. *et al.* Inconsistencies of echocardiographic criteria for the grading of aortic valve stenosis. *Eur Heart J.* **29**, 1043–1048 (2008).
6. Pibarot, P. & Dumesnil, J. G. Assessment of aortic stenosis severity: check the valve but don't forget the arteries! *Heart.* **93**, 780–782 (2007).
7. Eleid, M. F. *et al.* Survival by stroke volume index in patients with low-gradient normal EF severe aortic stenosis. *Heart.* **101**, 23–29 (2014).
8. Pibarot, P. Aortic stenosis: flow matters. *Heart.* **101**, 5–6 (2014).
9. Nishimura, R. A. *et al.* 2014 AHA/ACC guidelines for the management of patients with valvular heart disease: a report of the American college of cardiology/American heart association task force on practice guidelines. *J Am Coll Cardiol.* **63**, e57–e185 (2014).
10. Pierard, L. A. & Dulgheru, R. Evaluation of aortic stenosis: an update—including low-flow states, myocardial mechanics, and stress testing. *Curr Cardiol Rep.* **17**, 1–12 (2015).
11. Lancellotti, P. *et al.* Clinical outcome in asymptomatic severe aortic stenosis. *J Am Coll Cardiol.* **59**, 235–243 (2012).
12. Delgado, V. *et al.* Strain analysis in patients with severe aortic stenosis and preserved left ventricular ejection fraction undergoing surgical valve replacement. *Eur Heart J.* **30**, 3037–3047 (2009).
13. Small, E. M., Frost, R. J. A. & Olson, E. N. MicroRNAs add a new dimension to cardiovascular disease. *Circulation.* **121**, 1022–1032 (2010).
14. Thum, T. & Condorelli, G. Long noncoding RNAs and microRNAs in cardiovascular pathophysiology. *Circ Res.* **116**, 751–762 (2015).
15. Olson, E. N. MicroRNAs as therapeutic targets and biomarkers of cardiovascular disease. *Sci Transl Med.* **6**, 239ps3 (2014).
16. Derda, A. A. *et al.* Blood-based microRNA signatures differentiate various forms of cardiac hypertrophy. *Int J Cardiol.* **196**, 115–122 (2015).
17. Lang, R. M. *et al.* Recommendations for cardiac chamber quantification by echocardiography in adults: an update from the American society of echocardiography and the European association of cardiovascular imaging. *Eur Heart J Cardiovasc Imaging.* **16**, 233–270 (2015).
18. Hachicha, Z., Dumesnil, J. G. & Pibarot, P. Usefulness of the valvuloarterial impedance to predict adverse outcome in asymptomatic aortic stenosis. *J Am Coll Cardiol.* **54**, 1003–1011 (2009).
19. Lancellotti, P. *et al.* Risk stratification in asymptomatic moderate to severe aortic stenosis: the importance of the valvular, arterial and ventricular interplay. *Heart.* **96**, 1364–1371 (2010).
20. Marwick, T. H. *et al.* Recommendations on the use of echocardiography in adult hypertension: a report from the European association of cardiovascular imaging (EACVI) and the American society of echocardiography (ASE). *Eur Heart J Cardiovasc Imaging.* **16**, 577–605 (2015).
21. Voigt, J. U. *et al.* Definitions for a common standard for 2D speckle tracking echocardiography: consensus document of the EACVI/ASE/industry task force to standardize deformation imaging. *Eur Heart J Cardiovasc Imaging* **16**, 1–11 (2015).
22. Clavel, M. *et al.* Outcome of patients with aortic stenosis, small valve area, and low-flow, low-gradient despite preserved left ventricular ejection fraction. *J Am Coll Cardiol.* **60**, 1259–1267 (2012).
23. Dahl, J. S. *et al.* Development of paradoxical low-flow, low-gradient severe aortic stenosis. *Heart.* **101**, 1015–23 (2015).
24. Bergler-Klein, J. *et al.* Natriuretic peptides predict symptom-free survival and postoperative outcome in severe aortic stenosis. *Circulation.* **109**, 2302–2308 (2004).
25. Thum, T. *et al.* MicroRNA-21 contributes to myocardial disease by stimulating MAP kinase signalling in fibroblasts. *Nature.* **456**, 980–984 (2008).
26. Villar, A. V. *et al.* Myocardial and circulating levels of microRNA-21 reflect left ventricular fibrosis in aortic stenosis patients. *Int J Cardiol.* **167**, 2875–2881 (2013).
27. Fabiani, I. *et al.* Micro-RNA-21 (biomarker) and global longitudinal strain (functional marker) in detection of myocardial fibrotic burden in severe aortic valve stenosis: a pilot study. *J Transl Med.* **14**, 248 (2016).
28. Roncarati, R. *et al.* Circulating miR-29a, among other up-regulated microRNAs, is the only biomarker for both hypertrophy and fibrosis in patients with hypertrophic cardiomyopathy. *J Am Coll Cardiol.* **63**, 920–927 (2014).
29. Duisters, R. F. *et al.* MiR-133 and miR-30 Regulate connective tissue growth factor: implications for a role of microRNAs in myocardial matrix remodeling. *Circ Res.* **104**, 170–178 (2009).
30. García, R. *et al.* Circulating levels of miR-133a predict the regression potential of left ventricular hypertrophy after valve replacement surgery in patients with aortic stenosis. *J Am Heart Assoc.* **2**, e00021 (2013).
31. Carè, A. *et al.* MicroRNA-133 controls cardiac hypertrophy. *Nat Med.* **13**, 613–618 (2007).
32. Latronico, M. V. G., Costinean, S., Lavitrano, M. L., Peschle, C. & Condorelli, G. Regulation of cell size and contractile function by akt in cardiomyocytes. *Annals of the New York Academy of Sciences.* **1015**, 250–260 (2004).
33. Elia, L. *et al.* Reciprocal regulation of microRNA-1 and insulin-like growth factor-1 signal transduction cascade in cardiac and skeletal muscle in physiological and pathological conditions. *Circulation.* **120**, 2377–2385 (2009).
34. Magalhaes, M. A. *et al.* Outcome of left-sided cardiac remodeling in severe aortic stenosis patients undergoing transcatheter aortic valve implantation. *Am J Cardiol.* **116**, 595–603 (2015).

Acknowledgements

The project (lab assays) has been funded with PRA (Progetto di Ricerca di Ateneo) 2016 fundings, which are University (Public) Fundings yearly allocated to the most significant research projects, by a public multi-disciplinary condition.

Author Contributions

I.F., N.R.P. and V.D.B. conceived the study. FabianiIacopo and Pugliese Nicola Riccardo contributed equally to this work and are joint first authors. I.F., N.R.P., E.C., L.C., M.C.M., C. Scatena, C. Scopelliti, E.T., M.P., M.A., G.A.N., R.D.S., A.S.P. and V.D.B. took part to the definition of intellectual content. I.F., N.R.P., E.C., L.C., M.C.M., C. Scopelliti, E.T., M.P., M.A., G.A.N., R.D.S., A.S.P. and V.D.B. performed literature search. I.F., N.R.P., E.C., L.C., M.C.M. and C. Scatena have been involved in data acquisition and analysis. I.F., N.R.P., E.C., L.C., M.C.M. and C. Scatena wrote the main manuscript. Contributor Tantillo Elena created and checked bibliography. E.C., L.C. and M.C.M. created Tables 1–4 and Figure 1. Contributor E.C. is the corresponding author. Contributor V.D.B. supervised the study. All authors reviewed the manuscript.

Additional Information

Supplementary information accompanies this paper at <https://doi.org/10.1038/s41598-018-28246-8>.

Competing Interests: The authors declare no competing interests.

Publisher's note: Springer Nature remains neutral with regard to jurisdictional claims in published maps and institutional affiliations.



Open Access This article is licensed under a Creative Commons Attribution 4.0 International License, which permits use, sharing, adaptation, distribution and reproduction in any medium or format, as long as you give appropriate credit to the original author(s) and the source, provide a link to the Creative Commons license, and indicate if changes were made. The images or other third party material in this article are included in the article's Creative Commons license, unless indicated otherwise in a credit line to the material. If material is not included in the article's Creative Commons license and your intended use is not permitted by statutory regulation or exceeds the permitted use, you will need to obtain permission directly from the copyright holder. To view a copy of this license, visit <http://creativecommons.org/licenses/by/4.0/>.

© The Author(s) 2018